Template subtraction to remove CI stimulation artifacts in auditory steady-state responses in CI subjects

Hanne Deprez*, *Student Member, IEEE,* Robin Gransier, Michael Hofmann, Astrid van Wieringen, Jan Wouters, and Marc Moonen, *Fellow, IEEE*

***Abstract*—Objectives: Cochlear implant (CI) stimulation artifacts are currently removed from electrically evoked steady-state response (EASSR) measurements based on a linear interpolation (LI) over the artifact-contaminated signal parts. LI is only successful if CI stimulation artifacts are shorter than the interpulse interval, i.e. for contralateral channels and stimulation pulse rates up to 500 pulses per second (pps). The objective of this paper is to develop and evaluate a template subtraction (TS) method to remove continuous CI stimulation artifacts in order to accurately measure EASSRs.**

Methods: The template construction (TC) is based on an EEG recording containing CI stimulation artifacts but no synchronous neural response. The constructed templates are subtracted from the recording of interest. Response amplitudes and latencies are compared for the TS and LI method, and for different TC durations.

Results: The response amplitudes and latencies in contralateral channels are the same after TS and LI, as expected. In ipsilateral channels, response amplitudes and latencies are within the expected range only after TS. The TC duration can be reduced from 5 minutes to 1 minute without a significant change in response latency.

Conclusion: TS with a TC duration of only 1 minute allows to remove all CI stimulation artifacts in individual contra- and ipsilateral EEG recording channels.

***Index Terms*—Cochlear implant (CI), CI stimulation artifact removal, electrically evoked auditory steady-state responses (EASSR), template subtraction.**

I. Introduction

COCHLEAR implants (CIs) restore hearing in subjects with severe to profound sensorineural hearing loss. A CI bypasses the impaired cochlea by electrically stimulating the auditory nerve. The CI consists of three main parts: a sound processor which encodes incoming sound to electrical pulse stimulation patterns, a radiofrequency link which communicates between the CI's external and internal parts, and an electrode array consisting of 12–22 electrode contacts which is implanted into the cochlea. A CI also has one or two extra-cochlear electrodes, which are used as a reference in monopolar stimulation mode. This mode consumes less battery power than the bipolar stimulation mode, i.e., between two intra-cochlear stimulation electrodes, and it is therefore the standard mode used in the clinic [1]. Furthermore, in clinical settings, all CIs use high-rate stimulation, with pulse rates that are higher than 500 pulses per second (pps) [2].

Recently, there has been increasing interest in measuring the electroencephalogram (EEG) in CI subjects, both for automating CI fitting [3]–[5] and for investigating neural plasticity after cochlear implantation [6]–[10]. At CI activation and during audiological rehabilitation, several parameters have to be adjusted in the CI's sound processor, a process called CI fitting. The threshold (T) and maximum comfortable (C) stimulation levels are the main parameters that have to be set for each stimulation electrode. These are typically determined based on behavioral feedback from the CI subject, but could possibly be determined objectively and automatically with electrophysiological measures. For stimulation in monopolar mode, T levels vary less over stimulation electrodes than in bipolar mode, which is another reason that monopolar mode is generally used in clinical settings.

Objective threshold estimation based on responses at the auditory nerve and brainstem level has been investigated, but the obtained threshold levels are only moderately correlated with behavioral thresholds [11], [12]. These methods use low-rate stimulation, i.e., below 100 Hz, with larger T levels than high-rate stimulation [13]. Electrically evoked auditory steady-state responses (EASSRs) are neural responses elicited with periodic or modulated high-rate pulse trains. These narrow-band responses are obtained at the repetition or modulation frequency and can objectively be detected in the EEG based on frequency domain statistical tests [14]. It has been shown that electrophysiological thresholds obtained with modulated high-rate pulse trains correlate well with behavioral thresholds for stimulation in bipolar mode [4]. The current objective here is to investigate whether EASSRs to clinically used stimulation, e.g., high-rate pulse train stimulation in monopolar mode, could be used for objective threshold estimation.

Electrical stimulation also results in CI stimulation artifacts,

This research work was carried out in the frame of Research Project FWO nr. G.066213 'Objective mapping of cochlear implants', IWT O&O Project nr. 150432 'Advances in Auditory Implants: Signal Processing and Clinical Aspects', and KU Leuven Research Council CoE PFV/10/002 (OPTEC). The second author is supported by a Ph.D. grant by the Hermes Fund (141243).

Asterisk indicates corresponding author.

*H. Deprez is with Experimental ORL, Department of Neurosciences and with STADIUS Center for Dynamical Systems, Signal Processing and Data Analytics, Department of Electrical Engineering (ESAT), KU Leuven, Leuven, Belgium (e-mail: hanne.deprez@esat.kuleuven.be).

R. Gransier, M. Hofmann, A. van Wieringen and J. Wouters are with Experimental ORL, Department of Neurosciences, KU Leuven, Leuven, Belgium.

M. Moonen is with STADIUS Center for Dynamical Systems, Signal Processing and Data Analytics, Department of Electrical Engineering (ESAT), KU Leuven, Leuven, Belgium.

Manuscript received xxx; revised xxx.

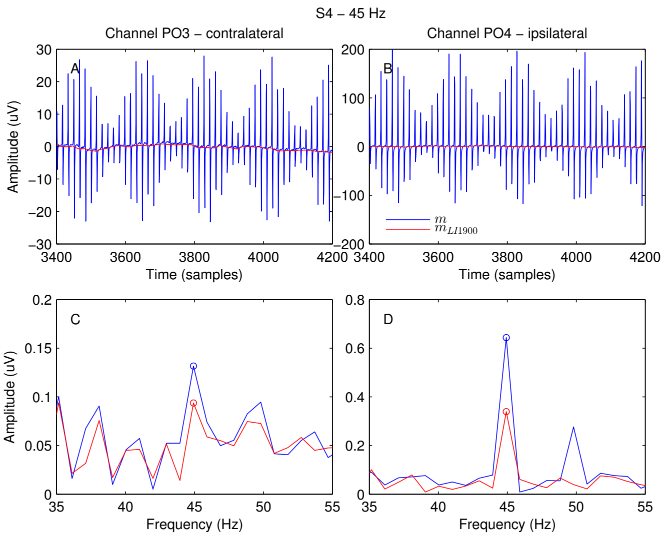

Fig. 1. Example of an EASSR, measured in subject S4, in contralateral channel PO_3 and ipsilateral channel PO_4, for stimulation with a 45 Hz amplitude modulated 500 pps pulse train (see Section II-A). An average epoch is shown in time and frequency domain (panel C and D), without CI stimulation artifact removal and with LI based CI stimulation artifact removal, denoted as m and $m_{LI_{1900}}$, respectively (panel A and B). CI stimulation artifact peak-to-peak amplitudes are about 50 μV and 300 μV in the contralateral and ipsilateral channel, respectively. The expected EASSR amplitudes are about $20-800$ nV [3], [5], which is 1000 times smaller than the CI stimulation artifact peak-to-peak amplitude. In the contralateral channel PO_3, CI stimulation artifacts are approximately symmetric and therefore have only a small component at the modulation frequency. This component is removed with LI_{1900} (panel C). The remaining EASSR has an amplitude of 94 nV. In the ipsilateral channel PO_4, CI stimulation artifacts are larger and less symmetric, and have a larger component at the modulation frequency (panel D). Even with LI_{1900}, the CI stimulation artifacts cannot completely be removed, because the CI stimulation artifacts are longer in duration than the interpulse interval of 2 ms. After LI, he component at the modulation frequency therefore has a larger amplitude in the ipsilateral than the contralateral channel, and consists both of EASSR and residual artifact. More information about the CI stimulation artifact characterization can be found in [17].

which obscure the neural responses. These CI stimulation artifacts may be present at the response frequency [3], [4] and can therefore not easily be removed with frequency domain filtering. The nature of the CI stimulation artifacts varies over subjects and depends on stimulation and recording parameters. CI stimulation artifacts are typically larger and longer in duration for monopolar mode stimulation than for bipolar mode stimulation [15], [16], and are therefore more difficult to remove. CI stimulation artifacts, shown in Figure 1 have been characterized in [17], for stimulation and recording parameters that are often used. A CI stimulation artifact typically consists of one or two large initial peak(s) and a slowly decaying tail.

A number of multichannel processing methods, based on principal component analysis (PCA), independent component analysis (ICA) or beamforming, have been investigated for CI stimulation artifact removal in transient EEG responses [18]–[23]. An ICA-based method has been developed in [24] for CI stimulation artifact removal in EASSRs. To our knowledge this is the only work evaluating multichannel methods for steady-state responses. Multichannel methods can employ spatial information about the neural response and the CI stimulation artifacts. However, they have the disadvantage that multichannel set-ups are more expensive to purchase than single channel set-ups, and more subject preparation time is required.

Several single channel methods for CI stimulation artifact removal have been investigated for transient [25]–[27] and steady-state responses [3], [4]. For EASSRs, the most successful method currently available is a linear interpolation (LI) method over each signal part that is contaminated with CI stimulation artifact. This method only works well if the CI stimulation artifacts are shorter than the interpulse interval. It has been shown recently that LI can remove CI stimulation artifacts from contralateral channels electrodes for stimulation in monopolar mode at pulse rates lower than or equal to 500 pps [5], [17]. For higher rates or for channels closer to the CI, the artifact tail has not completely decayed to the baseline level by the time the next pulse is started. Figure 1 illustrates that LI cannot completely remove the CI stimulation artifacts at ipsilateral recording channels.

Template subtraction (TS) methods have been developed in the context of transient EEG responses [27], but have not been considered for steady-state responses. The aim of this work is to develop a TS method for steady-state responses. The TS method can be applied to single channel data, which is an advantage for clinical applications such as objective CI fitting. Furthermore, the method is tailored to individual subjects and therefore copes well with intra- and intersubject variability, as a template is constructed for each channel and each subject separately. Finally, it is not assumed that CI stimulation artifacts are shorter than the interpulse interval (as for LI) or that they are similar in different recording channels (as for multichannel methods). We hypothesize that the TS method, contrary to the LI method, is able to remove CI stimulation artifacts from ipsilateral recording channels for high-rate stimulation in monopolar mode at suprathreshold stimulation levels.

However, it is not straightforward to apply the methods developed for transient responses to steady-state responses. For transient responses, typically the same stimuli are used for all presentations, while modulated pulse trains with varying stimulation pulse amplitudes are used for EASSRs. Therefore, a template should be constructed for each stimulation pulse amplitude, instead of a single template for one recurring stimulus. Furthermore, the steady-state nature of the stimulation and response imply that both continuously overlap. For transient responses, there is typically some delay between the occurrence of the CI stimulation artifacts and the event-related neural response. Therefore, even if the CI stimulation artifacts are not completely removed from the EEG signals, some information about the neural responses can still be obtained. For steady-state responses, even small residual CI stimulation artifacts can have a component at the modulation frequency, obscuring the event-related neural response. Consequently, the TS method should reduce the CI stimulation artifacts to a level below the brain noise level to reliably measure EASSRs.

The aim of this work is to develop and evaluate a TS method for EASSRs. The template construction (TC) is based on an EEG recording containing CI stimulation artifacts but no synchronous neural response. The constructed templates are subtracted from the recording of interest. Response amplitudes and latencies are compared for the TS and LI method, and for different TC durations.

II. Materials and methods

A CI stimulation artifact removal method based on TS was developed, which is described in Section II-B3. The TS method was compared to three other methods (no artifact removal and LI with two interpolation durations, see Sections II-B1 and II-B2) for part of the dataset collected by Gransier *et al* [5] (see Section II-A).

A. EASSR dataset

A part of the EASSR dataset described in [5] was used to evaluate the TS method. A brief description of the dataset follows.

The EASSRs were recorded for a wide range of modulation frequencies f_m, between 0 and 100 Hz, during either 2 or 3 recording sessions, to determine the most efficient modulation frequency for objective CI fitting. Amplitude modulated (AM) high-rate 500 pps pulse trains were presented at maximum comfort level to 6 post-lingually deafened subjects with a Cochlear Nucleus implant. Monopolar mode stimulation was used for all measurements, between intracochlear electrode 11 and the two extra-cochlear electrodes (MP1+2). The pulse rate was not an exact multiple of the modulation frequency. The pulse trains were modulated in amperes between the subject's unmodulated threshold level (T_u) and the modulated maximum comfortable level (C_m). Cochlear Nucleus implants are programmed in discrete current level units (CU) which are logarithmically related to current (in μA). All current levels between T_u and C_m were used for stimulation. The number of different stimulation pulse amplitudes (i.e., current levels) used was constant within subjects and varied between 20 and 89 over subjects. Within one recording, the stimulation pattern used was the same for each epoch. The distribution of stimulation pulse amplitudes used in the stimulation epoch of the $f_m = 42$ Hz recording of subject S1 is shown in panel A of Figure 2.

EEG signals were recorded during 5 minutes per condition with a 64-channel ActiveTwo Biosemi system, with a 8192 Hz sampling rate and 1638 Hz built-in low pass filter. Triggers were sent to the recording system at the start of each 1.024 s epoch. In the 30 – 50 Hz range for f_m, EASSRs were prominently present in all subjects. In the 80–100 Hz range for f_m, EASSRs could not effectively be measured in this pool of subjects, contrary to ASSRs in normal hearing subjects. More details can be found in [5].

Here, all recordings with modulation frequency between 30 and 50 Hz, recorded in session 1, were used for the evaluation of the TS method. Prominent responses were present in these recordings. Furthermore, per subject, one recording with a modulation frequency in the 70-100 Hz range (88 Hz for all subjects but S3, and 70 Hz for S3), also recorded in session 1, was selected for the template construction, see Section II-B3. This recording did not contain a significant response.

TABLE I

Recording channel selection per subject. As in [5], channels in the parietal-temporal and occipital region were selected. For each subject, channels corresponding to locations on top of the RF coil and channels with excessive noise levels were excluded.

	Ref	Contralateral	Ipsilateral
S1	C_z	CP_5, O_1, P_5, P_7, PO_3, PO_7, TP_7	CP_6, O_2, PO_4
S2	C_z	CP_5, O_1, P_5, P_7, P_9, PO_3, PO_7, TP_7	CP_6, O_2, PO_4
S3	C_z	CP_6, O_2, P_6, P_8, PO_4, PO_8, TP_8	CP_5, O_1, P_5
S4	Fp_z	CP_5, O_1, P_5, P_7, P_9, PO_3, PO_7, TP_7	PO_4, O_2
S5	Fp_z	CP_5, O_1, P_5, P_7, P_9, PO_3, PO_7, TP_7	PO_4, O_2
S6	C_z	CP_6, O_2, P_6, P_8, P_{10}, PO_4, PO_8, TP_8	CP_5, O_1, P_5, PO_3

B. Data processing

The raw data signals $x[t, c]$, with t the time index and c the channel index, were stored in a matrix $\in \mathbb{R}^{N_t \times N_c}$, with N_t and N_c the number of time samples and channels, respectively. The signals were re-referenced offline to either the C_z or Fp_z recording channel (see Table I), depending on the spatial distribution of the subject's CI stimulation artifact [5], i.e.,

$$x^r[t, c] = x[t, c] - x[t, c_{ref}] \tag{1}$$

where c_{ref} refers to either C_z or Fp_z.

A set of specifically interesting recording channels in the parietal-temporal and occipital regions ($CP_{5/6}$, $TP_{7/8}$, $P_{5/6}$, $P_{7/8}$, $P_{9/10}$, $PO_{3/4}$, and $PO_{7/8}$) was selected for analysis. The same set as in [5] was used. For each subject, channels corresponding to locations on top of the RF coil and channels with excessive noise levels were excluded. The set of selected channels for each subject is included in Table I. Raw data signals were also averaged for the set of selected contra- and ipsilateral channels, resulting in two additional fictitious channel signals $\hat{c}_{\text{contra}}$ ($x[t, c_{contra}]$) and $\hat{c}_{\text{ipsi}}$ ($x[t, c_{ipsi}]$), and hence N_c became equal to $N_c + 2$.

Four CI stimulation artifact removal methods were used as described below: no artifact removal (NO), LI with interpolation duration $d = 1.1$ ms (LI_{1000}), LI with $d = 2.0$ ms (LI_{1900}) and template subtraction (TS).

1) No artifact removal (NO): First, the first-order trend $x^{trend}[t, c]$ of each channel $x^r[t, c]$, $c = 1 \ldots N_c$, was calculated with a 0.5 s sliding window and then subtracted.

$$x^d[t, c] = x^r[t, c] - x^{trend}[t, c] \tag{2}$$

The resulting de-trended data signals $x^d[t, c]$ were then split in 1.024 s epochs based on the trigger signal at the start of each epoch, and 5% of the epochs were rejected based on their peak-to-peak amplitude to eliminate excessive movement, ocular, and muscle artifacts. The epoch signals were stored in a three-dimensional tensor $\mathcal{X}[t', e, c] \in \mathbb{R}^{N_{t'} \times N_e \times N_c}$, with $N_{t'}$ the number of time samples in one epoch and N_e the number of epochs. Next, the Fourier transform $\overline{\mathcal{X}}[f, e, c]$ of the epoch signals was calculated for each epoch $e = 1 \ldots N_e$ and channel $c = 1 \ldots N_c$.

$\overline{\mathcal{X}}[f, e, c]$ was then used to determine the amount of synchronous and non-synchronous activity at the modulation frequency as follows. The synchronous activity (i.e., the neural response and CI stimulation artifacts) and non-synchronous activity (i.e., the brain background noise) were compared to decide whether significant synchronous activity is present. The synchronous activity was calculated for each channel as the average component at the modulation frequency $\overline{m}[f_m, c]$, averaged over epochs.

$$\overline{m}[f_m, c] = \text{mean}(\overline{\mathcal{X}}[f_m, e, c])_e \tag{3}$$

The response amplitude and phase were determined as the absolute value and angle of this average component.

$$\begin{aligned} A[f_m, c] &= |\overline{m}[f_m, c]| \\ \theta[f_m, c] &= \angle\overline{m}[f_m, c] \end{aligned} \tag{4}$$

This component can consist of both neural response and CI stimulation artifacts, with some residual brain background noise superimposed depending on the number of epochs averaged. For each channel, the brain background noise level was determined as the standard deviation of the component at the modulation frequency over epochs, divided by the square root of the number of epochs N_e.

$$N[f_m, c] = \frac{std(\overline{\mathcal{X}}[f_m, e, c])_e}{\sqrt{N_e}} \tag{5}$$

The Hotelling T^2 test [28] was used to compare the average real and imaginary components at the modulation frequency to the brain background noise level to determine whether significant synchronous activity is present. Response amplitude and phase were used further on to compare the four methods.

2) Linear interpolation (LI$_{1000}$ and LI$_{1900}$): After re-referencing (1), a linear interpolation was applied between each pre-stimulus sample t_{pre} and post-stimulus sample t_{post} that are both assumed to be free from CI stimulation artifact.

$$x^l[t, c] = x^r[t_{pre}, c] + \frac{x^r[t_{post}, c] - x^r[t_{pre}, c]}{t_{post} - t_{pre}}(t - t_{pre}) \qquad t_{pre} < t < t_{post} \qquad c = 1 \dots N_c \tag{6}$$

The time between the pre- and post-stimulus samples is referred to as the interpolation duration $d = t_{post} - t_{pre}$. The maximum possible interpolation duration is the interpulse interval, which is the inverse of the pulse rate, in this case 2 ms. The pre-stimulus samples were always chosen at 0.1 ms before the start of a stimulation pulse, the post-stimulus samples were chosen at either 1 ms (LI$_{1000}$) or 1.9 ms (LI$_{1900}$) after the start of a stimulation pulse. Further processing followed the steps outlined above in Section II-B1, i.e., detrending (2), averaging (3), EASSR (4) and brain background noise (5) calculation, and testing for significant synchronous activity with the Hotelling T^2 test. It has been shown that this method is indeed capable of removing the CI stimulation artifacts from contralateral recording channels for stimulation rates up to 500 pps [5], [17].

3) Template subtraction (TS): The TS method used two recordings: (1) a template construction (TC) recording $x_{TC}[t, c]$ which contained no neural response and was used to construct a template of the CI stimulation artifact for every stimulation pulse amplitude (i.e., current level in CU); and (2) the recording of interest $x[t, c]$ from which the templates were subtracted. A recording without any synchronous neural response was used for the TC, to ensure that the templates only model the CI stimulation artifacts. It is of major importance that the tail of each CI stimulation artifact is modeled accurately; since any inaccuracies due to inadequate modeling of the initial artifact peaks can still be removed by LI.

After re-referencing (1), a 0.5 s sliding window first-order de-trending (2) was applied to $x_{TC}[t, c]$ and $x[t, c]$. The resulting signals were split in epochs based on the trigger signal, 5% of the epochs were rejected based their peak-to-peak amplitude. The remaining epoch signals were stored as $\mathcal{X}_{TC}[t', e, c]$ and $\mathcal{X}[t', e, c]$. Next, all signals were averaged over epochs, resulting in the mean epochs $m_{TC}[t', c]$ and $m[t', c]$.

$$m_{TC}[t', c] = \text{mean}(\mathcal{X}_{TC}[t', e, c])_e \tag{7}$$

$$m[t', c] = \text{mean}(\mathcal{X}[t', e, c])_e \tag{8}$$

For the TC recording, a template for each stimulation pulse amplitude was determined based on the mean epoch. First, the mean epoch matrix $m_{TC}[t', c]$ was rearranged into tensor $\mathcal{M}_{TC}[p, \widehat{t}, c] \in \mathbb{R}^{N_p \times N_{\widehat{t}} \times N_c}$, with N_p the number of pulses in one epoch and $N_{\widehat{t}}$ the number of samples per stimulation pulse (in this case $\lfloor \frac{8192 \text{ samples/s}}{500 \text{ pps}} \rfloor = 16$ samples/pulse). The rows of $\mathcal{M}_{TC}[p, \widehat{t}, c]$ contained the CI stimulation artifact following stimulation pulse p. The set of unique stimulation pulse amplitudes was called P_u. Then, all CI stimulation artifacts corresponding to pulses with the same amplitude were averaged, resulting in a template $\mathcal{T}[p_u, \widehat{t}, c]$ for each stimulation pulse amplitude p_u and for each channel c.

$$\forall p_u \in P_u : \mathcal{T}[p_u, \widehat{t}, c] = \text{mean}(\mathcal{M}_{TC}[p = p_u, \widehat{t}, c])_p \tag{9}$$

Next, the pulse templates were rearranged based on the stimulation pulse amplitude pattern used in the recording of interest, resulting in an epoch template $T_{epoch}[t', c]$.

Finally, this epoch template was subtracted from the mean epoch of the recording of interest (8), resulting in $m_{TS}[t', c]$.

$$m_{TS}[t', c] = m[t', c] - T_{epoch}[t', c] \tag{10}$$

A LI was then applied to each channel of $m_{TS}[t', c]$, because the initial peaks of the CI stimulation artifacts are not always adequately sampled with the relatively low sampling rate, which is also shown in panel B and C of Figure 2.

We chose $t_{pre} = 0.1$ and $t_{post} = 1$ ms or equivalently $d = 1.1$ ms, as this is a conservative value for the interpolation duration that definitely removes all the initial peaks of the CI stimulation artifacts for the sample rate used in these measurements.

The resulting mean epoch $m_{TS,LI_{1000}}[t', c]$ and its Fourier transform $\overline{m}_{TS,LI_{1000}}[f, c]$ were used to evaluate the response

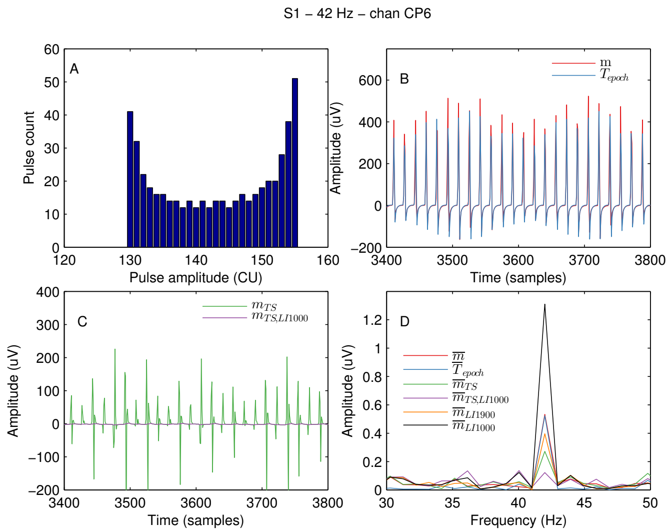

Fig. 2. Illustration TS method for subject S1 in ipsilateral channel CP_6 for stimulation with an 42 Hz AM 500 pps pulse train. (A) Histogram of stimulation pulse amplitudes used within one stimulation epoch. All stimulation pulse amplitudes p_u between T_u and C_m are used for stimulation. A template $T[p_u, \widehat{t}, c]$ is constructed for each of these stimulation pulse amplitudes p_u. (B) Part of a mean epoch without CI stimulation artifact removal $m[t', c]$ (red) and constructed template $T_{epoch}[t', c]$ (blue), in the time domain. The templates are similar to the original signal, although the artifact peaks are not adequately modeled. (C) Mean epoch after TS $m_{TS}[t', c]$ (green), and after TS and LI_{1000} $m_{TS,LI_{1000}}[t', c]$ (purple), in the time domain. After TS, the mean epoch still contains some residual CI stimulation artifacts, due to inadequate modeling of the artifact initial peak. These are removed with LI_{1000}. (D) Mean epoch in frequency domain, without artifact removal $\overline{m}[f, c]$ (red), CI stimulation artifact template $\overline{T}_{epoch}[f, c]$ (blue), mean epoch after TS $\overline{m}_{TS}[f, c]$ (green), after TS and LI_{1000} $\overline{m}_{TS,LI_{1000}}[f, c]$ (purple), after LI_{1000} $\overline{m}_{LI_{1000}}[f, c]$ (orange) and after LI_{1900} $\overline{m}_{LI_{1900}}[f, c]$ (black). The component at f_m is different for $\overline{m}_{LI_{1000}}$ than for $\overline{m}_{TS,LI_{1000}}$, indicating that the template subtraction does have a beneficial effect.

properties. For each channel c, the amplitude and phase of the synchronous activity were calculated as the absolute value and angle of $\overline{m}_{TS,LI_{1000}}[f_m, c]$, as in (4). The non-synchronous activity is determined from the original epoch signals $\mathcal{X}[t', e, c]$ as in (5). The original epoch signals, without CI stimulation artifact removal, were used to calculate the brain background noise level, as the presence of CI stimulation artifacts should not have any impact on the non-synchronous activity.

An example is shown in Figure 2, for the $f_m = 42$ Hz recording of S1 at the ipsilateral channel CP_6.

C. Evaluation of CI stimulation artifact removal methods

EASSR amplitudes and latencies were determined and used to confirm that the TS method effectively attenuates the CI stimulation artifacts below the noise level of the recordings. The LI_{1000} results were included because the same interpolation duration was used in the TS method, and were presented in order to rule out that any effects seen may be due to the LI only.

1) EASSR amplitude: EASSR amplitudes $A[f_m, c]$ were determined after LI and TS and compared for the individual contralateral channels and the channel $\hat{c}_{\text{contra}}$.

The EASSR amplitude difference between any of the first three methods on the one hand and the TS method on the other hand, relative to the noise amplitude $N[f_m, c]$, was determined as follows:

$$\Delta A[f_m, c] = \frac{A[f_m, c]_{No/LI_{1000}/LI_{1900}} - A[f_m, c]_{TS}}{N[f_m, c]} \quad (11)$$

Negative values indicate that the response amplitude after TS was larger than for the other method. Amplitude differences were considered small when these were within the noise level, i.e., ΔA between -1 and 1.

For each subject, the median value (and interquartile range (IQR)) of ΔA over modulation frequencies and channels, was determined. Furthermore, the median value (and IQR) over subjects, modulation frequencies and channels was also calculated.

2) Response latency: If the neural response is significantly larger than the brain background noise, the response phases $\theta[f_m, c]$ should decrease linearly with increasing modulation frequency f_m in the 30–50 Hz range [5], [29]. The non-zero slope of this linear decrease is related to the response latency. For CI stimulation artifact dominated measurements, response phases are stable at multiples of 180 degrees, regardless of the modulation frequency [3]–[5]. The slope of the $\theta(f_m)$ curve thus indicates whether the measurement is either neural response or CI stimulation artifact dominated, as it is related to the response latency.

A first-order polynomial was fit to the $\theta(f_m)$ curve, based on a least squares procedure. The response latency was calculated as the additive inverse of the slope, for all individual channel signals and for the channels $\hat{c}_{\text{contra}}$ and $\hat{c}_{\text{ipsi}}$. In a causal system, the response latency should be positive. However, the fit is not constrained to negative slopes, i.e., positive response latencies. Therefore, in case of CI stimulation artifact dominated measurements, the response phase does not necessarily decrease with increasing modulation frequency, resulting in positive slopes and a negative response latency. For the channels $\hat{c}_{\text{contra}}$ and $\hat{c}_{\text{ipsi}}$, a Wilcoxon signed-rank test was used to determine whether response latencies differed significantly between LI_{1900} and TS. For contralateral channels, response latencies were compared after LI_{1900} and TS as these should be very similar. For ipsilateral channels, response latencies of individual channels were compared to the expected median values of $44.2 (IQR = 6.8)$ ms. These expected values were taken from [5].

The response latency differences between different methods were calculated as:

$$\Delta RL = RL_{No/LI_{1000}/LI_{1900}} - RL_{TS} \quad (12)$$

where RL represents the response latency. Negative values mean that the response latency for TS is larger than for the other method, indicating that the CI stimulation artifacts are better removed with the TS method.

D. Influence of TC duration

The described method used a full recording $x^{TC}[t, c]$ with $0.95 * 300 = 285$ epochs to construct the CI stimulation artifact templates, which could result in excessive EEG recording

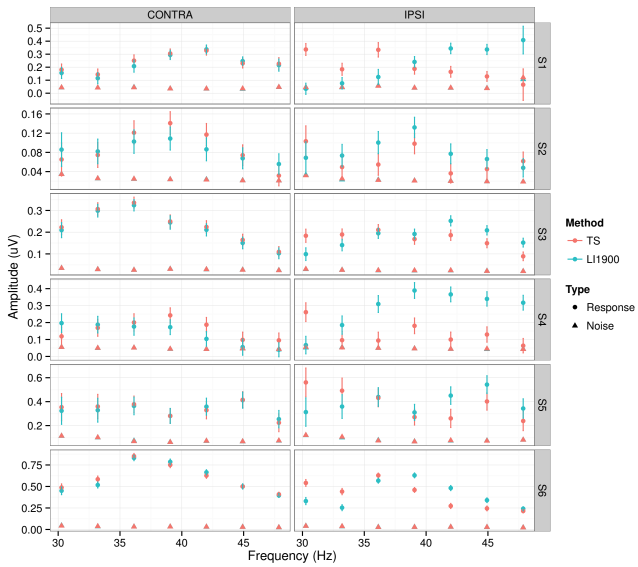

Fig. 3. EASSR amplitudes are similar after LI and TS for the channel $\hat{c}_{\text{contra}}$ in all subjects. In the ipsilateral channel $\hat{c}_{\text{ipsi}}$, EASSR amplitudes are generally smaller for TS than for LI_{1900}, except for the lowest modulation frequencies. Error bars represent the noise level.

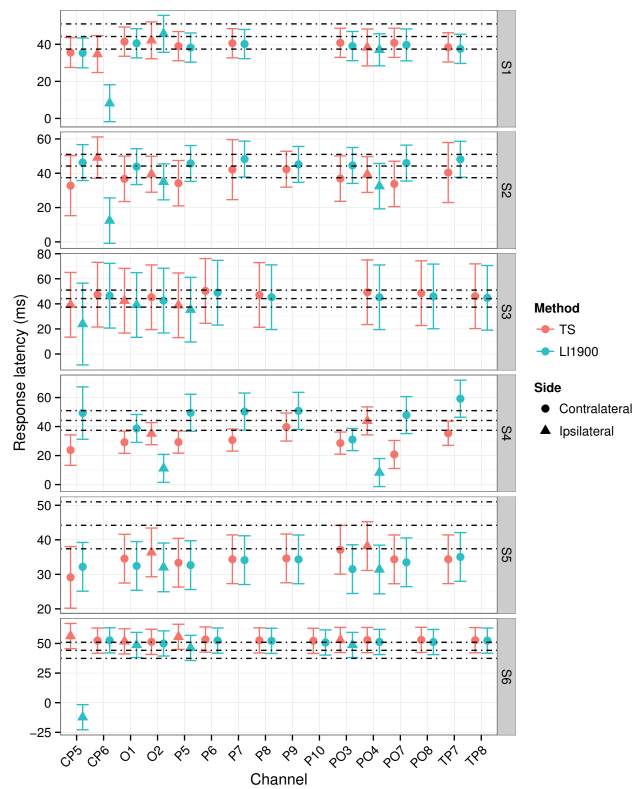

Fig. 4. EASSR latencies per recording channel for LI and TS. Response latencies are small for some ipsilateral channels in most subjects, but are within the expected range after TS. Response latencies are calculated from a first order fit of the $\theta(f_m)$ curve. Error bars correspond to the 95% confidence intervals of this fit. The horizontal lines indicate the range of expected latencies, and correspond to the median ($\pm$ IQR) values found in [5].

times. Therefore, the TC recording duration was varied from 60 to 270 epochs, in steps of 30 epochs, to investigate its influence on the response amplitude and latency values. A Friedman ANOVA was used to test whether the TC duration has a significant influence on the obtained response latency.

E. Software and statistical analysis

All data processing was done in MATLAB R2013a. R (v3.0.2) was used for statistical analysis, with significance level $\alpha = 0.05$.

III. Results

A. Response properties

1) EASSR amplitude: EASSR amplitudes observed in the channels $\hat{c}_{\text{contra}}$ and $\hat{c}_{\text{ipsi}}$ are shown in Figure 3 for each individual subject. For the channel $\hat{c}_{\text{contra}}$, EASSR amplitude differences after LI_{1900} and TS are within the noise level. Therefore amplitudes after LI_{1900} are not significantly different from amplitudes after TS. For the channel $\hat{c}_{\text{ipsi}}$, EASSR amplitudes are generally smaller for TS than for LI_{1900}, except for the lower modulation frequencies ($30 - 33$ Hz). The amplitude differences ΔA between the first three methods and TS, as defined in Equation (11), are included in Table II.

2) Response latency: Response latencies for individual channels are included in Figure 4. For contralateral recording channels, median response latencies (and IQRs) are 40.4(16.8) ms, 48.2(18.8) ms, 45.3(11.1) ms, and 39.3(12.9) ms without artifact removal, after LI_{1000}, after LI_{1900} and after TS, respectively. For ipsilateral recording channels, median response latencies (and interquartile ranges) are $-3.6(47.9)$ ms, 5.6(14.6) ms, 32.5(26.7) ms, and 39.4(10.8) ms without artifact removal, after LI_{1000}, after LI_{1900} and after TS, respectively. The Wilcoxon signed-rank test did not show a significant difference in response latency between LI_{1900} and TS ($p > 0.05$) for the channel $\hat{c}_{\text{contra}}$. However, for channel $\hat{c}_{\text{ipsi}}$, a significant difference in response latency is found after LI_{1900} and TS ($p = 0.03$). For most subjects, response latencies are within the expected range [4], [5] for all channels after TS, whereas latencies are smaller than expected for ipsilateral channels after LI_{1900}. For subject S4, response latencies after TS are rather small, although latencies are larger than after LI_{1900} in ipsilateral channels. TS is thus able to remove more CI stimulation artifact from ipsilateral channels than LI.

Response latency differences, as defined in Equation (12), comparing all available methods to the proposed TS method, are included in Table II.

B. Influence of TC duration

The influence of the TC duration on the response latency in the channels $\hat{c}_{\text{contra}}$ and $\hat{c}_{\text{ipsi}}$ is shown in Figure 5. Already for short TC durations of 60 (TS_{60}) or 90 (TS_{90}) epochs, the obtained latencies are very close to the ones obtained with 270 (TS_{270}) epochs TC duration, indicating that short TC durations are sufficient for adequate CI stimulation artifact removal. Response latencies are compared for TS_{60}, TS_{90}, and TS_{270} using a Friedman ANOVA. No significant difference

TABLE II
RESPONSE PROPERTIES: RESPONSE AMPLITUDE DIFFERENCE (ΔA) BETWEEN METHODS DIVIDED BY NOISE AMPLITUDE; AND RESPONSE LATENCY DIFFERENCE (ΔRL) BETWEEN METHODS. MEDIAN(IQR) OVER MODULATION FREQUENCIES (FOR AMPLITUDE DIFFERENCES), AND SELECTED INDIVIDUAL CONTRA- AND IPSILATERAL CHANNELS (SEE TABLE I) FOR EACH SUBJECT, AND OVER SUBJECTS.

		S1	S2	S3	S4	S5	S6	all
ΔA ([])								
Contralateral								
	No vs TS	0.3(2.7)	1.0(4.0)	0.0(1.5)	-0.2(1.7)	0.0(0.4)	-0.6(3.7)	0.0 (1.9)
	LI_{1000} vs TS	0.0(1.2)	0.6(2.8)	0.5(1.8)	0.3(2.1)	0.0(0.7)	0.1(1.9)	0.1(1.6)
	LI_{1900} vs TS	-0.2(0.9)	-0.2(1.0)	-0.3(0.3)	-0.5(1.5)	-0.1(0.5)	-0.2(1.1)	-0.2(0.9)
Ipsilateral								
	No vs TS	0.4(4.8)	10.2(19.3)	2.0(4.9)	6.5(6.9)	-0.1(5.4)	10.9(19.5)	3.6(11.8)
	LI_{1000} vs TS	4.6(9.0)	5.6(16.8)	7.2(12.8)	17.5(5.2)	4.6(4.9)	9.5(20.3)	7.1(15.2)
	LI_{1900} vs TS	0.5(3.8)	0.3(0.9)	0.4(3.0)	4.1(2.5)	0.6(2.0)	0.7(6.4)	0.5(3.8)
ΔRL (ms)								
Contralateral								
	No vs TS	-9.0(1.7)	17.5(19.1)	-4.9(1.8)	11.2(4.0)	-1.4(0.4)	-2.8(1.1)	-2.1(13.3)
	LI_{1000} vs TS	0.4(1.9)	15.7(7.3)	3.3(1.5)	-34.0(40.5)	0.9(2.8)	1.0(2.6)	1.6(5.4)
	LI_{1900} vs TS	-0.8(0.4)	7.7(4.8)	-1.8(1.3)	19.9(13.5)	-0.5(1.1)	-1.1(1.0)	-0.4(8.8)
Ipsilateral								
	No vs TS	4.2(27.7)	-46.4(4.0)	-46.0(26.2)	-43.9(4.3)	-2.5(8.6)	-58.5(15.8)	-43.3(51.0)
	LI_{1000} vs TS	-33.0(7.5)	-30.5(12.0)	-33.2(15.1)	-37.3(4.7)	-21.5(4.3)	-49.2(17.7)	-33.0(19.7)
	LI_{1900} vs TS	-1.3(15.0)	-6.8(16.1)	-3.5(6.0)	-29.8(5.8)	-5.6(1.2)	-6.8(20.2)	-6.8(20.5)

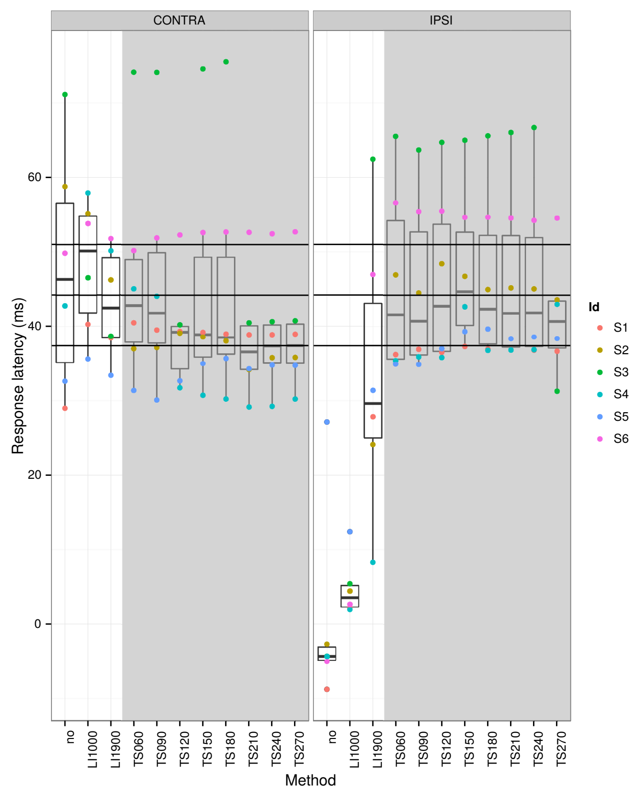

Fig. 5. EASSR apparent latencies for LI and TS, for channels $\hat{c}_{\text{contra}}$ and $\hat{c}_{\text{ipsi}}$: influence of TC duration. No significant difference is found between TS_{060}, TS_{090}, and TS_{270} in either channel.

in response latency is found in the $\hat{c}_{\text{contra}}$ ($\chi^2(2) = 1.33, p = 0.51$) or $\hat{c}_{\text{ipsi}}$ channel ($\chi^2(2) = 0.33, p = 0.85$).

IV. DISCUSSION

EEG signals measured during continuous CI stimulation are distorted by CI stimulation artifacts, which may also be present at the neural response frequency. CI stimulation artifacts have very large amplitudes and their contribution at the response frequency may be several orders of magnitude larger than the neural response itself. Hofmann *et al* showed that CI stimulation artifacts can effectively be attenuated using LI, for low- and high-rate stimulation in bipolar mode [3], [4]. In [5], EASSRs to 500 pps modulation pulse trains were measured for a large range of modulation frequencies with stimulation in monopolar mode, and responses free of CI stimulation artifacts were found and analyzed in contralateral recording channels. In previous work [17], we have shown that CI stimulation artifacts can be characterized based on their duration, which is shorter than the interpulse interval at contralateral channels, for stimulation with 500 pps pulse trains stimulated in monopolar mode. Furthermore, it was shown that the reference channel may have an influence on the artifact characteristics.

It has thus been shown that CI stimulation artifacts can be removed from contralateral recording channels using LI, for stimulation pulse rates up to 500 pps [5], [17]. The our knowledge, non of the available methods is capable of attenuating the CI stimulation artifact below the noise level at ipsilateral recording channels.

In this work, we developed and evaluated an alternative TS based artifact removal method, by constructing artifact templates for each stimulation pulse amplitude and subtracting these from a recording of interest. We hypothesized that such a (single channel) method would be capable of modeling subject- and channel-specific CI stimulation artifacts without imposing an assumption on the artifact duration. The artifact templates are constructed based on a recording that does not contain a significant EASSR, to ensure that the artifact template only models the artifact and does not contain EASSR components. The method was applied to EEG recordings containing significant EASSRs in response to suprathreshold stimulation levels.

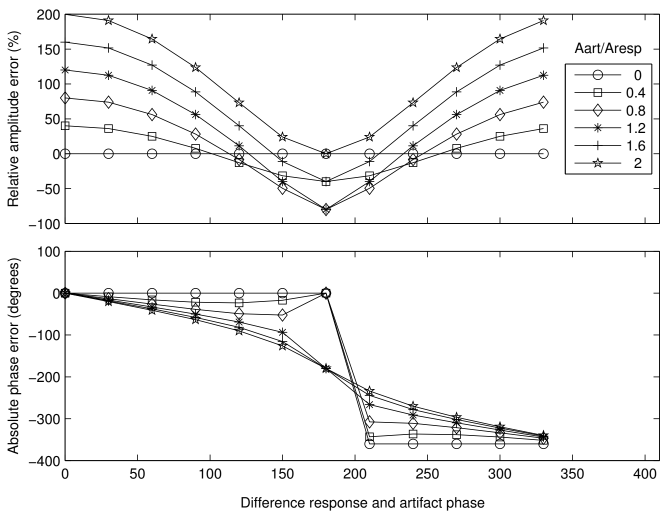

Fig. 6. Relative amplitude and absolute phase error in function of the difference in response and artifact phase. Generally, larger artifacts result in larger amplitude and phase errors. Amplitude errors are largest when response and artifact are in phase or around 180° out of phase. Phase errors are generally smaller for these phase differences, and are largest when response and artifact are $100 - 150°$ or $200 - 250°$ out of phase.

A. Results and interpretation

1) Contralateral: In the contralateral recording channels, the EASSR is dominant compared to the relatively small contribution of the CI stimulation artifact, as observed in Table II. Median normalized response amplitude errors were between -1 and 1 for all methods. However, the IQR of the error between LI_{1900} and TS seems to be smaller than for the other methods. The obtained amplitudes for LI_{1900} and TS are more similar than for any of the remaining methods (no and LI_{1000} vs TS).

As shown in Section III-A2, median response latencies were very similar for all four methods, but IQRs were smaller after LI_{1900} and TS than after NO and LI_{1000}, indicating that LI_{1900} and TS still remove more CI stimulation artifacts.

The same observation can be made based on the response latency differences: median differences were rather small between NO, LI_{1000}, LI_{1900} on the one side and TS on the other side. For most subjects, IQRs of the response latency differences were smaller when LI_{1900} and TS were compared, than for NO and LI_{1000} vs TS.

2) Ipsilateral: In the ipsilateral channels, EEG signals were clearly dominated by CI stimulation artifacts when no artifact removal or LI_{1000} is applied. In the $\hat{c}_{\text{ipsi}}$ channel, EASSR amplitudes are generally smaller for TS than for LI_{1900}, see Figure 3, except for the lowest modulation frequencies. We observed that CI stimulation artifact and EASSR are in phase at these modulation frequencies. We modeled the observed amplitude and phase error, for varying artifact-response amplitude ratios and artifact-response phase differences, see Figure 6. Amplitude errors are largest when artifact and response are in phase, and increase with higher residual artifact levels. It is thus likely that this result reflects some residual artifact in the 30 and 33 Hz recordings in some subjects.

Response amplitude differences between TS and NO or LI_{1000} ranged from -0.1 to 17.5 times the noise level (median value). This indicates that response amplitudes were up to 17.5 times the noise level larger for LI_{1000} and NO than for TS. Furthermore, very large IQRs were observed. The median response amplitude difference between LI_{1900} and TS was within the noise level for most subjects, but the IQR of this error was variable over subjects, up to 6.4 times the noise level. This indicates that amplitude differences for all methods compared to TS can be quite large for ipsilateral recording channels.

The median response latencies of -3.6 and 5.6 ms obtained with NO and LI_{1000} methods were rather small, compared to the expected value of 44.2 ms. This indicates that the EEG signals were dominated by the CI stimulation artifacts. Note that a negative apparent latency is not physiologically possible, but is a result of the first-order fit on artifact dominated measurements. The median response latency of 32.5 ms for LI_{1900} was within the expected range, but the IQR of 26.7 ms was rather large compared to the expected value of 6.8 ms. This indicates that conditions (e.g., subjects, recordings, and recording channels) exist for which the LI_{1900} does not remove all CI stimulation artifacts. The values obtained after TS (median = 39.4 ms, IQR = 10.8 ms) were in line with the expectations.

The median response latency differences of NO and LI_{1000} compared to TS were more than 20 ms, for most subjects. After LI_{1900}, appropriate latencies were obtained for some subjects, but not all, while the latencies were within the expected range for all subjects after TS, see Figure 4.

The LI_{1000} method was unable to remove all CI stimulation artifacts from the EEG signals, while reliable response latencies were obtained with the TS method. Importantly, the main contribution of the method is thus in the adequate modeling of the CI stimulation artifact tail, and not in the LI after the template subtraction.

B. Significance

Good results were obtained in the two fictitious averaged channels $\hat{c}_{\text{contra}}$ and $\hat{c}_{\text{ipsi}}$, as shown in Figures 3 and 5. Furthermore, response properties for individual recording channels are included in Figures 4 and Table II. It is interesting to see that reliable response properties were obtained in all individual recording channels as well.

In clinical environments, multichannel systems are often not available or impractical. Because good results were obtained in individual contralateral and ipsilateral recording channels, objective CI fitting methods based on single channel recordings could be developed.

A possible disadvantage of the method is the need of a response-free recording for template construction. We showed that the duration of the recording used for template construction can be reduced to 1 minute, without significant changes in obtained response latencies. The additional recording time could thus be reduced to 1 minute, provided that stimulation is between the same minimum and maximum level in both recordings. In case several stimulation levels are tested, 1 minute extra recording time is needed per tested stimulation level.

Artifact-free EEG signals at ipsilateral channels are of major importance for lateralization studies, that e.g., look into the reorganization or development of the auditory pathway in long-term hearing deprived subjects or infants and children with CIs. In case of bilateral CI stimulation, the LI method is incapable of providing useful information, as ipsilateral channels contain large and long CI stimulation artifacts that cannot be removed. The results presented in the present study indicate the feasibility of removing CI stimulation artifacts at all (including ipsilateral) channels using the TS method. Furthermore, for source localization purposes, it is important that artifact-free EEG signals are obtained over the entire scalp with small spatial resolution. Using the LI method with unilateral CI stimulation, at least a quarter of the channels is excluded, because these are too close to the CI. In case of bilateral CI stimulation, even more channels are unavailable.

C. Future work

First, future work should focus on improvements of the proposed method. It should be investigated whether additional template construction recordings could be omitted: CI stimulation artifact templates could possibly be constructed based on recordings that have to be acquired during the protocol. Models describing the scaling behaviour of pulse templates for increasing pulse amplitudes could be used to make generalizations of CI stimulation artifact properties and behaviour. The EEG signals may still contain some residual artifact after template subtraction, and methods could be developed to remove this residual CI stimulation artifact.

Furthermore, the performance of the TS method should be investigated for EEG signals with smaller or no neural responses than the ones present in the 40 Hz range dataset used in this study. In this study, only recordings to suprathreshold stimulation at C level were considered. However, the EASSRs amplitudes vary between 40 and 1048 nV in the pool of subjects tested in this study. Therefore, we would argue that a representative range of 40 Hz EASSR amplitudes has already been tested. In infants and children, it may be necessary to use modulation frequencies in the 80 Hz range to measure EASSRs. During neonatal hearing screening, infants are usually tested with 80 Hz range modulated stimuli, as attention effects and sleep do not play a role at these modulation frequencies [30], [31]. To our knowledge, up to date, no study has examined the effect of modulation frequency on EASSRs in infants and children with a CI yet. In NH subjects, it has been shown that EASSR amplitudes are generally smaller in the 80 Hz range, compared to the 40 Hz range, with reduced brain noise levels as well [29]. During CI fitting procedures, EASSRs near and below threshold have to be measured reliably. It is crucial that all CI stimulation artifacts are removed from these recordings to prevent false detections and incorrect threshold estimations. When the CI stimulation artifacts are not attenuated below the noise level, the stimulation artifact is dominant for low EASSR amplitudes, causing large amplitude and phase errors on the observed synchronous component, as shown in Figure 6.

V. Conclusion

A template subtraction method for CI stimulation artifact removal from EEG signals recorded during continuous CI stimulation has been developed. A template is constructed for every stimulation pulse amplitude based on a template construction recording (TC), containing CI stimulation artifacts but no neural response. This template is then subtracted from the recording of interest.

Response properties are similar for LI_{1900} and TS, at individual contralateral recording channels and for the channel $\hat{c}_{\mathrm{contra}}$. For LI_{1900}, response amplitudes are too large and latencies are too small at individual ipsilateral recording channels and for the channel $\hat{c}_{\mathrm{ipsi}}$. Only the TS method is able to remove the CI stimulation artifacts and results in reliable response amplitudes and latencies. A TC duration of only 1 minute is sufficient to construct adequate templates that result in reliable response properties after subtraction.

Future work will evaluate how well the TS method works on EEG signals with smaller neural responses that are more easily dominated by CI stimulation artifacts. Alternative methods that eliminate any residual CI stimulation artifacts after TS will also be developed and evaluated.

Acknowledgment

Special thanks also goes out to Robert Luke and Tom Francart for their valuable input and feedback on this work.

References

[1] T. Zwolan, P. R. Kileny, C. Ashbaugh, and S. A. Telian, "Patient performance with the Cochlear Corporation '20+2' implant: bipolar vs monopolar activation," *American Journal of Otolaryngology*, vol. 17, no. 1996, pp. 717–723, 1996.

[2] J. Wouters, H. J. McDermott, and T. Francart, "Sound coding in cochlear implants: From electric pulses to hearing," *IEEE Signal Processing Magazine*, vol. 32, no. 2, pp. 67–80, 2015.

[3] M. Hofmann and J. Wouters, "Electrically evoked auditory steady state responses in cochlear implant users." *Journal of the Association for Research in Otolaryngology : JARO*, vol. 11, no. 2, pp. 267–282, 2010.

[4] ——, "Improved electrically evoked auditory steady-state response thresholds in humans," *JARO - Journal of the Association for Research in Otolaryngology*, vol. 13, no. 4, pp. 573–589, 2012.

[5] R. Gransier, H. Deprez, M. Hofmann, M. Moonen, A. V. Wieringen, and J. Wouters, "Auditory steady-state responses in cochlear implant users: effect of modulation frequency and stimulation artifacts," *Hearing Research*, vol. 335, pp. 1–43, 2016.

[6] A. Sharma, M. F. Dorman, and A. J. Spahr, "A sensitive period for the development of the central auditory system in children with cochlear implants: Implications for age of implantation," *Ear Hear*, vol. 23, no. 6, pp. 532–539, 2002.

[7] A. Sharma, P. M. Gilley, M. F. Dorman, and R. Baldwin, "Deprivation-induced cortical reorganization in children with cochlear implants," *International journal of audiology*, vol. 46, no. 9, pp. 494–499, 2007.

[8] A. Sharma, A. A. Nash, and M. Dorman, "Cortical development, plasticity and re-organization in children with cochlear implants," *Journal of Communication Disorders*, vol. 42, no. 4, pp. 272–279, 2009.

[9] P. M. Gilley, A. Sharma, and M. F. Dorman, "Cortical reorganization in children with cochlear implants," *Brain Research*, vol. 1239, no. 1999, pp. 56–65, 2008.

[10] K. A. Gordon, D. D. E. Wong, and B. C. Papsin, "Bilateral input protects the cortex from unilaterally-driven reorganization in children who are deaf," *Brain*, vol. 136, no. 5, pp. 1609–1625, 2013.

[11] C. J. Brown, M. L. Hughes, B. Luk, P. J. Abbas, a. Wolaver, and J. Gervais, "The relationship between EAP and EABR thresholds and levels used to program the nucleus 24 speech processor: data from adults." *Ear and hearing*, vol. 21, no. April 2000, pp. 151–163, 2000.

[12] M. L. Hughes, C. J. Brown, P. J. Abbas, a. a. Wolaver, and J. P. Gervais, “Comparison of EAP thresholds with MAP levels in the nucleus 24 cochlear implant: data from children.” *Ear and hearing*, vol. 21, no. 2, pp. 164–174, 2000.

[13] C. M. McKay, K. Chandan, I. Akhoun, C. Siciliano, and K. Kluk, “Can ECAP measures be used for totally objective programming of cochlear implants?” *JARO - Journal of the Association for Research in Otolaryngology*, vol. 14, no. 6, pp. 879–890, 2013.

[14] R. A. Dobie and M. J. Wilson, “A Comparison of t test, F test, and coherence methods of detecting steady-state auditory-evoked potentials, distortion-product otoacoustic emissions, or other sinusoids,” *Journal Acoustical Society of America*, vol. 100, no. 4, pp. 54–71, 1996.

[15] M. L. Hughes, C. J. Brown, and P. J. Abbas, “Sensitivity and specificity of averaged electrode voltage measures in cochlear implant recipients.” *Ear and hearing*, vol. 25, no. 5, pp. 431–446, 2004.

[16] X. Li, K. Nie, F. Karp, K. L. Tremblay, and J. T. Rubinstein, “Characteristics of stimulus artifacts in EEG recordings induced by electrical stimulation of cochlear implants,” *3rd International Conference on Biomedical Engineering and Informatics*, pp. 799–803, 2010.

[17] H. Deprez, R. Gransier, M. Hofmann, A. van Wieringen, J. Wouters, and M. Moonen, “Characterization of cochlear implant artifacts in electrically evoked auditory steady-state responses,” *Biomedical Signal Processing and Control*, 2016, In press.

[18] P. M. Gilley, A. Sharma, M. Dorman, C. C. Finley, A. S. Panch, and K. Martin, “Minimization of cochlear implant stimulus artifact in cortical auditory evoked potentials.” *Clinical Neurophysiology*, vol. 117, no. 8, pp. 1772–1782, 2006.

[19] B. A. Martin, “Can the acoustic change complex be recorded in an individual with a cochlear implant? Separating neural responses from cochlear implant artifact.” *Journal of the American Academy of Audiology*, vol. 18, no. 2, pp. 126–40, 2007.

[20] D. D. E. Wong and K. A. Gordon, “Beamformer suppression of cochlear implant artifacts in an electroencephalography dataset.” *IEEE Transactions on Biomedical Engineering*, vol. 56, no. 12, pp. 2851–2857, 2009.

[21] N. Castañeda-Villa and C. J. James, “Independent component analysis for auditory evoked potentials and cochlear implant artifact estimation,” *IEEE Transactions on Biomedical Engineering*, vol. 58, pp. 348–354, 2011.

[22] F. C. Viola, M. De Vos, J. Hine, P. Sandmann, S. Bleeck, J. Eyles, and S. Debener, “Semi-automatic attenuation of cochlear implant artifacts for the evaluation of late auditory evoked potentials.” *Hearing research*, vol. 284, pp. 6–15, 2012.

[23] I. Akhoun, C. M. McKay, and W. El-deredy, “Electrically evoked compound action potential artifact rejection by independent component analysis: technique validation,” *Hearing research*, vol. 302, pp. 60–73, 2013.

[24] H. Deprez, M. Hofmann, A. van Wieringen, J. Wouters, and M. Moonen, “Cochlear implant artifact rejection in electrically evoked auditory stead y state responses,” in *European Signal Processing Conference*, vol. 002, 2014.

[25] J. B. Fallon, D. R. F. Irvine, and R. K. Shepherd, “Cochlear implants and brain plasticity,” *Hearing Research*, vol. 238, no. 1-2, pp. 110–117, 2008.

[26] L. M. Friesen and T. W. Picton, “A method for removing cochlear implant artifact.” *Hearing research*, vol. 259, pp. 95–106, 2010.

[27] M. McLaughlin, A. L. Valdes, R. B. Reilly, and F.-G. Zeng, “Cochlear Implant Artifact Attenuation in Late Auditory Evoked Potentials: A Single Channel Approach,” *Hearing research*, vol. 302, pp. 84–95, 2013.

[28] H. Hotelling, “The Generalization of Student’s Ratio,” *The Annals of Mathematical Statistics*, vol. 2, pp. 360–378, 1931.

[29] T. W. Picton, M. S. John, A. Dimitrijevic, and D. Purcell, “Human auditory steady-state responses.” *International journal of audiology*, vol. 42, no. 2012, pp. 177–219, 2003.

[30] M. Aoyagi, T. Kiren, Y. Kim, Y. Suzuki, T. Fuse, and Y. Koike, “Optimal modulation frequency for amplitude-modulation following response in young children during sleep.” *Hearing research*, vol. 65, no. 1-2, pp. 253–61, 1993.

[31] E. C. Levi, R. C. Folsom, and R. A. Dobie, “Amplitude-modulation following response (AMFR): Effects of modulation rate, carrier frequency, age, and state,” *Hearing Research*, vol. 68, no. 1, pp. 42–52, 1993.